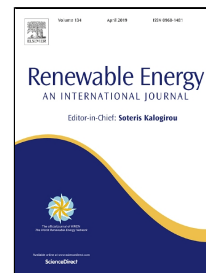# Accepted Manuscript

Solid catalysts obtained from wastes for FAME production using mixtures of refined palm oil and waste cooking oils

Edgar M. Vargas, Márcia C. Neves, Luís A.C. Tarelho, Maria I. Nunes

Please cite this article as: Edgar M. Vargas, Márcia C. Neves, Luís A.C. Tarelho, Maria I. Nunes, Solid catalysts obtained from wastes for FAME production using mixtures of refined palm oil and waste cooking oils, *Renewable Energy* (2019), doi: 10.1016/j.renene.2019.01.048

Solid catalysts obtained from wastes for FAME production using mixtures of refined palm oil and waste cooking oils

Edgar M. Vargas[a], Márcia C. Neves[b], Luís A. C. Tarelho[c], Maria I. Nunes[d,*]

[a] Dep. of Chemical Engineering, University Jorge Tadeo Lozano, Bogotá, Colombia | edgar.vargas@utadeo.edu.co

[b] Dep. of Chemistry and CICECO, University of Aveiro, 3810-193 Aveiro, Portugal | mcneves@ua.pt

[c] Centre for Environmental and Marine Studies, Dep. of Environment and Planning, University of Aveiro, 3810-193 Aveiro, Portugal | ltarelho@ua.pt

[d] Centre for Environmental and Marine Studies, Dep. of Environment and Planning, University of Aveiro, 3810-193 Aveiro, Portugal | isanunes@ua.pt, isanunes24@gmail.com

* Corresponding author. Tel.: +351 924 406 201

E-mail address: isanunes@ua.pt; isanunes24@gmail.com (M.I. Nunes)

Postal Code: 3810 – 193 Aveiro, Portugal.

1   **Solid catalysts obtained from wastes for FAME production using**

2   **mixtures of refined palm oil and waste cooking oils**

3   Edgar M. Vargas[a], Márcia C. Neves[b], Luís A. C. Tarelho[c], Maria I. Nunes[c,*]

4   [a] Dep. of Chemical Engineering, University Jorge Tadeo Lozano, Bogotá, Colombia

5   [b] Dep. of Chemistry and CICECO, University of Aveiro, Portugal

6   [c] Centre for Environmental and Marine Studies, Dep. of Environment and Planning,
7   University of Aveiro, Portugal

8

9   **Abstract**

10   More than 95% of biodiesel production feedstocks come from edible oils, however it may

11   cause some problems such as the competition of land use between food production

12   and biodiesel production. The waste cooking oils (WCO) are an alternative feedstock for

13   biodiesel production; its usage reduces significantly the cost of biodiesel production and has

14   environmental benefits, e.g., a waste recovery instead of its elimination. This work aims to

15   produce a low-cost efficient solid catalyst for fatty acid methyl esters (FAME) production

16   using mixtures of refined palm oil (RPO) and WCO. Four low cost catalysts were prepared

17   (biomass fly ashes, natural dolomite rock, chicken eggshells and polyethylene terephthalate

18   - PET), characterized (by SEM, EDX, XRD, BET, FT-IR and Hammett indicators) and tested

19   regarding their performance in FAME production. The maximum yield of FAME achieved

* Corresponding author. Tel.: +351 924 406 201

E-mail address: isanunes@ua.pt; isanunes24@gmail.com (M.I. Nunes)

Postal Code: 3810 − 193 Aveiro, Portugal.

20 was around 96%wt. for biomass fly ashes catalyst at 60 ºC, 9:1 (mol/mol) of methanol to oil

21 mixture, 10%wt. catalyst to oil mixture, over 180 min in batch reactor. The results point out

22 for promising bifunctional catalysts able to achieve also conversion of free fatty acids up to

23 100% using mixtures of RPO and WCO.

24

1   Introduction

28 Energy is a basic requirement for human existence. The total world energy consumption will

29 grow by 56% between 2010 and 2040 [1]. In the current situation, the foremost amount of

30 primary and useful energy is supplied by the conventional fossil fuel resources, such as

31 gasoline, liquefied petroleum gas, diesel fuel, and natural gas. However, the use of fossil

32 fuels has several influences on the environment, such as large greenhouse gas emissions, acid

33 rain, resources depletion, etc. In addition to serious environmental issues, dwindling reserves

34 of crude oil, fluctuating petroleum fuel prices, have made today's need to find alternative

35 "green" sources of energy, which are sustainable, environmentally compatible, economically

36 competitive, and easily available. One of the most promising sources is biodiesel, an

37 alternative diesel fuel derivate from renewable sources with high quality, which allows the

38 replacement of fossil diesel oil [2]. Usually the biodiesel production is a catalyzed process

39 where alkali or acid compounds are used, respectively, for the conversion of triglycerides

40   (transesterification reaction) and free fatty acids – FFA (esterification reaction) into fatty acid

41   methyl esters (FAME), when methanol is used in the synthesis. In line with the circular

42   economy principles, the development of solid catalysts from waste sources could be a

43   promising way for reducing the environmental burdens of the process and the production

44   costs. Some research works [3,4] have focused on the exploitation of waste materials (e.g.

45   shells, ashes, rocks and bones), due to their abundance and low cost, for solid catalysts

46   preparation.

47   Globally, the cost of production has been the main barrier in commercializing biodiesel. In

48   the literature, it is consensual that the oily feedstock is the major contributor, about 80% [5],

49   for the total production costs. The use of edible oils sparks concern in terms of food security

50   while the non-edible oils need additional pre-treatment steps. On the other hand, the wide

51   availability of edible oils guarantees the supply while the alternative of non-edible oils is

52   subject to an intermittent supply [6].

53   The waste cooking oils (WCO) are some vegetable oils that have been previously used for

54   frying or cooking and can constitute an additional source of raw material for biodiesel

55   production. This feedstock can be two to three times cheaper that virgin vegetable oils [7].

56   Furthermore, it is generally accepted that reusing used cooking oil for human consumption

57   is harmful to health [8] and the WCO is difficult to manage.

58   In the research that focuses on the biodiesel production process there is a new trend of

59   bifunctional heterogeneous catalysts that, if used properly, can catalyze both

60   transesterification and esterification reactions simultaneously. This ability is due to the

61   presence of both basic and acidic sites on the same catalysts. Additionally, this kind of

3

62 catalysts can be modified to introduce/improve certain physicochemical properties needed to

63 handle with low grade feedstocks (e.g. some WCO). Usually these raw-materials have high

64 FFA and/or water contents, which are undesirable for transesterification reaction [9].

65

66 This work aims to produce an efficient solid bifunctional catalyst from residual materials for

67 FAME production using mixtures of refined palm oil (RPO) and WCO in different ratios.

68 Thus, this work tackles two current environmental concerns giving an alternative for

69 recovering some important wastes fluxes (WCO, fly ashes, dolomite, eggshells and

70 polyethylene terephthalate (PET) plastic garbage containers), aligned with the principles of

71 circular economy, and for reducing the dependence of fossil fuel, through the production of

72 biofuel mainly from waste materials feedstocks.

73 # 2   Materials and Methods

74 Solid catalysts were prepared and characterized in terms of some of their chemical, physical

75 and structural properties. The raw-material for FAME synthesis consisted of a mixtures of

76 WCO and RPO in different ratios. The adopted procedures are described in next sections.

77 The experimental plan for assessing the performance of the catalysts in the FAME production

78 will be presented later as well as the analytical methods used.

79 ## 2.1   Materials

80 Waste cooking oil for FAME production was provided by a local collecting company (Bioils)

81 in Bogotá, Colombia. The WCO was pre-treated by filtration and heating (at 110°C for 1h)

4

82   to remove suspended particles and traces of water, respectively. The RPO was purchased at

83   a local store in Bogotá. The solid waste materials for catalyst preparation were obtained from

84   the following sources:

85   ▪   biomass fly ashes – collected at the electrostatic precipitator of a thermal power-plant

86   using residual forest biomass (derived from eucalyptus) as fuel, located in the Centre

87   Region of Portugal;

88   ▪   natural dolomite rock- the mining industry in Colombia;

89   ▪   eggshells- several restaurants of Bogotá;

90   ▪   PET- plastic bottles picked from garbage containers at the University Jorge Tadeo

91   Lozano, Bogotá.

92   All the chemicals used were analytical grade except n-hexane (GC grade) and methyl

93   heptadecanoate (analytical standard) from Sigma-Aldrich and Merck.

94   2.2   Oil mixtures (RPO and WCO) characterization

95   Five feedstocks were prepared using different mass ratios of RPO and WCO: M1 (100%

96   RPO), M2 (75% RPO, 25% WCO), M3 (50% RPO, 50% WCO), M4 (25% RPO, 75% WCO)

97   and M5 (100% WCO).

98   These mixtures were characterized in terms of: acid value (NTC 218 [10]), density (NTC 336

99   [11]), saponification number (NTC 335 [12]), viscosity (ASTM D445 and ASTM D446

100   [13,14]), and moisture content (Karl Fisher, Coulometer 831-Metrohm). The saponification

101   number (*SN*) was used to calculate the molecular mass (*MW*) according to Eq. 1[5].

5

102
$$MW = \frac{56.1 \times 1000 \times 3}{SN} \qquad (1)$$

103 The FFA content was calculated from the acid value (AV, mgKOH/g) using Eq. 2 [5]

104
$$FFA = \frac{AV}{2} \qquad (2)$$

105

2.3 Catalysts preparation and characterization

107 Eight catalysts were prepared using low cost feedstocks, implementing the procedures

108 summarized in Table 1. The sulfonation or the addition of silicon to some catalysts aimed to

109 enhance their acid strength.

110 **Table 1:** Solid catalysts preparation procedures.

Catalyst reference		Preparation procedure
Biomass fly ash	FAD	Dry at 120°C for 5h.
	FAC	Calcine FAD at 700°C for 5h.
Natural dolomite rock	Dolomite C	Mill and sieve at 45μm and calcine at 800°C for 2h.
	Dolomite CSC	Impregnate dolomite C with H_2SO_4 2M for 6h at room temperature. Then, filter and dry for 12h at 110°C. Finally, calcine at 500°C for 4h.
Eggshells	CaO-SiO$_2$	Wash with water and dry at 120°C for 3h. Then, sieved at 63μm and calcine at 800°C for 4h. Impregnate with Na_2SiO_3 0.4 M aqueous solution at room temperature for 4h. Finally dry at 100°C for 12h and calcine at 800°C for 4h.
	CaO-S-SiO$_2$	Impregnate CaO-SiO$_2$ with H_2SO_4 2M for 6h at room temperature, dry at 110°C for 12h and calcine at 500°C for 3h.

6

PET	CA-PET	Reduce (cut) the PET containers to small pieces ($<1cm^2$) and heat 10°C/min for 2h from room temperature up to 450°C under a nitrogen atmosphere. Impregnate the resulting product with H_2SO_4 98% (1.5:1 v/w, H_2SO_4: PET) at 150°C for 2h. Then, wash with water and dry at 120°C for 6h. Mill and sieve at 106μm, and finally dry at 105°C for 24h.
	CA-PET-S	Impregnate CA-PET with fuming sulfuric acid (5:1v/w, H_2SO_4:CA-PET) at 150°C for 10h under a nitrogen atmosphere. Wash with water (until no sulfate ions are detected, using turbidimetric method) and dry at 105°C for 24h.

111

112   The solid catalysts were characterized in terms of: (i) crystallographic structures, by powder

113   X-ray (XRD, PAN analytical Empyrean X-ray diffractometer equipped with Cu-Kα radiation

114   source λ= 1.54178Å at 45kV/ 40mA); (ii) surface area, pore size and pore volume, by

115   Brunauer-Emmet-Teller sorption isotherm (BET, using N_2 at -196°C in Micromeritics ASAP

116   2020); (iii) surface morphology and quantitative elemental composition analysis, by surface

117   scanning electron microscopy (SEM, using FEG-SEM Hitachi S4100 microscope operated

118   at 25kV) and energy dispersive X-ray spectroscopy (EDX, using a HR-FESEM Hitashi SU-

119   70 operated at 15kV, equipped with a Bruker Quantax 400 EDS system); (iv) surface

120   functional species by Fourier transform infrared (FTIR, Agilent CARY 630 with wave

121   number range from 400 to 4000cm^{-1}); and (v) basic and acid strength by using Hammett

122   indicators (indicators for basic strength: neutral red (pKa = 6.8), bromothymol blue (pKa =

123   7.2), phenolphthalein (pKa = 9.3), indigo carmine (pKa = 12.2) and 2,4-dinitroaniline (pKa

124   = 15.0); indicators for acid strength: bromothymol blue (pKa = 7.2), neutral red (pKa = 6.8),

125   bromocresol purple (pKa = 6.1), bromocresol green (pKa = 4.7) and bromophenol blue (pKa

126   = 3.8)). The latter method was carried out by dispersing about 25mg of the sample in 5.0mL

127 of a solution of Hammett indicators (0.5mg of indicator in 10mL of methanol for basic

128 strength or 10mL of benzene for acid strength), and left for 2h in order to attain the

129 equilibrium. After reaching equilibrium, the color on the catalyst and solution were

130 identified.

131 **2.4 FAME synthesis**

132 The experiments for FAME production were carried out in batch reactor (in stainless steel,

133 1L of capacity, equipped with temperature control and mechanical agitator) at 60ºC, 9:1

134 (mol/mol) of methanol to oil mixture, 10%wt. catalyst to oil mixture and over 180min. After

135 the pre-defined reaction time, for each essay, the catalyst and methanol were separated from

136 the reaction mixture by centrifugation and evaporation, respectively. Then, the supernatant

137 was placed into a separating funnel over 12h for phase separation. The upper layer was dry

138 with anhydrous sodium and weighed. The resulting mixture, hereafter is so-called purified

139 final mixture, was analyzed by gas chromatography for FAME determination and was titrated

140 with a KOH solution for final acid value quantification [10].

141 The Shimadzu G-C 2014 chromatograph was equipped with a flame ionization detector and

142 a capillary column SGEBP-20 60m x 0.25mm i.d. x 0.25μm film thickness with a stationary

143 phase of polyethylene glycol; the carrier gas was helium with a flow rate of 16.7mL/min and

144 a pressure of 36.1psi; the injector (AOC-20i) was operated at 200ºC and an injection volume

145 of 2.0μL in Split mode. Methyl heptadecanoate was used as internal standard and hexane the

146 solvent. The content of methyl esters was calculated based on the standard method UNE-EN

147 ISO 14103:2011 [15] and expressed as concentration of FAME using the Eq. 3:

8

$$C = \frac{\sum A - A_{EI}}{A_{EI}} \times \frac{W_{EI}}{W}$$

148
(3)

149 Where C is the concentration of FAME in the purified final mixture (w/w), $\sum A$ is the total

150 peak areas of the methyl ester from C_{14} until $C_{24:1}$, A_{EI} is the peak area corresponding to

151 methyl heptadecanoate, W_{EI} is the mass (mg) of methyl heptadecanoate used and W is the

152 mass (mg) of the sample used in the analysis.

153 The catalysts performance was expressed in terms of FAME yield, Eq. 4, and FFA

154 conversion, Eq. 5 [16-17].

$$\text{FAME yield}\,(\%) = \frac{C \times \text{Total mass of purified final mixture}}{\text{Mass of oil used in the experiment}} \times 100$$

155
(4)

$$\text{FFA conversion}\,(\%) = \left(1 - \frac{AV_f}{AV_i}\right) \times 100$$

156
(5)

157 Where AV_i and AV_f correspond to the acid value of the initial oil mixture and of the purified

158 final mixture, respectively.

159 **3 Results and discussion**

160 **3.1 Oil mixtures characterization**

161 The results of the characterization of the oil mixtures prepared for this study are shown in

162 Table 2.

9

163 **Table 2:** Properties of the oil mixtures used.

	Mixture reference				
	M1	**M2**	**M3**	**M4**	**M5**
%WCO	0	25	50	75	100
%RPO	100	75	50	25	0
Moisture (%wt.)	0.067 ± 0.010	0.141 ± 0.017	0.170 ± 0.003	0.177 ± 0.013	0.197 ± 0.012
Density (g/mL)	0.908 ± 0.008	0.907 ± 0.004	0.913 ± 0.010	0.905 ± 0.007	0.906 ± 0.003
AV (mgKOH/g)	0.307 ± 0.004	1.249 ± 0.061	2.458 ± 0.082	3.873 ± 0.088	4.934 ± 0.252
FFA (%wt.)	0.172 ± 0.0048	0.622 ± 0.0512	1.240 ± 0.012	1.917 ± 0.048	2.453 ± 0.056
MW (g/mol)	843.152 ± 9.522	875.173 ± 10.285	864.038 ± 9.208	855.507 ± 3.69	857.825 ± 4.014
Viscosity (mm²/s)	14.902 ± 0.193	17.069 ± 0.137	17.122 ± 0.123	17.717 ± 0.150	19.185 ± 0.392

164

165 The properties of the mixture M1 (i.e., 100% RPO) are similar to those reported by Jibrail et

166 al. [18] and by Singh et al., [19]. Concerning the waste cooking oils properties, they are quite

167 dependent of the vegetable oil feedstocks and their frying practices and conditions. The WCO

168 (M5) used in this work has properties similar to those reported by Wan et al. [20] and Man

169 et al. [21] and it can be categorized as yellow grease (FFA <15%) [22].

170 Regarding the mixtures prepared with RPO and WCO, one observes that the density and the

171 molecular weight are not affected by the blending ratio. On the other hand, the properties

172 related to acidity of the mixtures (*AV* and FFA) rise significantly as the percentage of WCO

173 increases in the blend. The water content and the viscosity are properties that increase slightly

174 by increasing the WCO percentage in the blend.

175 **3.2 Catalysts characterization**

10

176 The solid catalysts prepared by the methods shown in Table 1 were characterized in terms of

177 some textural properties such as surface area, crystalline structure, but also their basic and

178 acid strength, etc. The results are shown and discussed below.

179 **3.2.1 BET surface area and Hammett indicators analyses**

180 The BET surface area, pore volume, pore diameter, basic and acid strength of catalysts are

181 shown in Table 3.

182 **Table 3:** Textural properties of the catalysts prepared in this work.

Catalyst	Specific surface area (m^2/g)	Pore volume (cm^3/g)	Pore diameter (Å)	Basic strength	Acid strength
FAD	9.0280	0.01055	77.188	$9.3 \leq pKa < 12.2$	$6.8 \leq pKa < 7.2$
FAC	5.1750	0.00791	101.849	$9.3 \leq pKa < 12.2$	$6.8 \leq pKa < 7.2$
Dolomite C	12.0113	0.04145	136.908	$12.2 \leq pKa < 15$	$6.8 \leq pKa < 7.2$
Dolomite CSC	15.2617	0.05291	113.689	$9.3 \leq pKa < 12.2$	$6.1 \leq pKa < 6.8$
CaO-SiO$_2$	6.6112	0.01285	56.874	$7.2 \leq pKa < 9.3$	$3.8 \leq pKa < 4.7$
CaO-S-SiO$_2$	12.6773	0.04330	109.925	$9.3 \leq pKa < 12.2$	$6.8 \leq pKa < 7.2$
CA-PET	1105.2	0.85871	14.983	ND	$6.1 \leq pKa < 6.8$
CA-PET-S	624.3	0.54221	14.871	ND	$3.8 \leq pKa < 4.7$

183 ND – not detected

184 The calcination of fly ashes seems to reduce the surface area (ca 40%) and pore volume (ca

185 25%), which can be due to sintering of the compounds on the solid matrix surface [24].

186 Nevertheless, this thermal treatment does not affect both basic and acid strength of this

187 catalysts. Both ash based catalysts have an intermediate basic strength ($9.3 \leq pKa < 12.2$) and

188 a low acid strength ($6.8 \leq pKa < 7.2$).

11

189 The sulfonation of Dolomite increases both surface area (ca 30%) and pore volume (ca 30%),

190 but reduces the pore diameter (ca 20%). These physical changes may have effects on the

191 performance of these materials in the catalysis of FAME production reactions. On one hand,

192 higher surface area and pore volume will have a positive effect on the catalysis, but on the

193 other hand, a decrease of pore diameter increases the diffusion limitations especially for

194 molecules having long alkyl chain [25]. Jacobson et al. [26] identified the pore structure as

195 the primary requirement for an ideal solid catalyst in the biodiesel production (via

196 transesterification) since a typical triglyceride molecule has a diameter of approximately

197 58Å. As foreseen, sulfonating the Dolomite C increases its acid strength ($6.8 \leq$ pKa <7.2 to

198 $6.1 \leq$ pKa <6.8) and decreases the basic strength ($12.2 \leq$ pKa <15 to $9.3 \leq$ pKa <12.2), values

199 close to those found by Boonyawan et al. [27]. However, Dolomite CSC has both acid and

200 basic strength which, a priori, gives it a bifunctional character.

201 The sulfonation of CaO-SiO$_2$ catalyst enhances considerably the three textural properties:

202 surface area, pore volume and pore diameter but decreases the acid strength ($3.8 \leq$ pKa <4.7

203 to $6.8 \leq$ pKa <7.2) and increases the basic strength ($7.2 \leq$ pKa <9.3 to $9.3 \leq$ pKa <12.2). The

204 effect of sulfonation and calcination on these strengths could be due to the formation of new

205 phases of basic character such as calcium sulfate and calcium silicate [28].

206 In regard to the catalysts prepared from PET both have an acid character being CA-PET-S

207 the strongest ($3.8 \leq$ pKa <4.7), and the basic strength was not detected in none. The acid

208 character of this carbon catalyst may promote the esterification reaction of FFA but not the

209 transesterifcation of triglycerides [29, 30]. The sulfonation treatment performed on the PET

210 catalyst reduced its specific surface area (ca 44%) and pore volume (ca 37%), which should

211 be ascribed to the modification of a large number of – SO_3H groups in the carbon framework.

212 In short, all catalysts prepared in this work could be classified as mesoporous catalysts since

213 the pore diameters are within the intermediate range (20 - 500Å) [31], except for the

214 carbonaceous catalysts (PET) which is microporous (< 20Å). This feature may influence the

215 catalysts' performance in the transesterification reaction since, as stated before, a typical

216 triglyceride molecule has a diameter of around 58Å. Hence, as larger are the porous higher

217 is the accessibility of those molecules to the inner pore structure network.

218 **3.2.2 SEM and EDX analyses**

219 The SEM images for characterizing the morphological characteristics and EDX for elemental

220 analysis or chemical characterization of the catalysts were obtained. Figure 1 shows the

221 morphological and the elemental composition of FAD and FAC catalysts. All particles of

222 both ash catalysts have uniform distribution of agglomerates with irregular shapes, and the

223 morphological sizes of the particles were reduced by the calcination treatment (Figure 1

224 a&e), possibly due to sintering processes, which decreases the surface area [32,33]. The

225 results of EDX show as predominant elements in these catalysts: Ca, Mg, Si, Al, O, K, S,

226 Na, Cl and P. These elements remained on the solid surface after calcination, as shown in

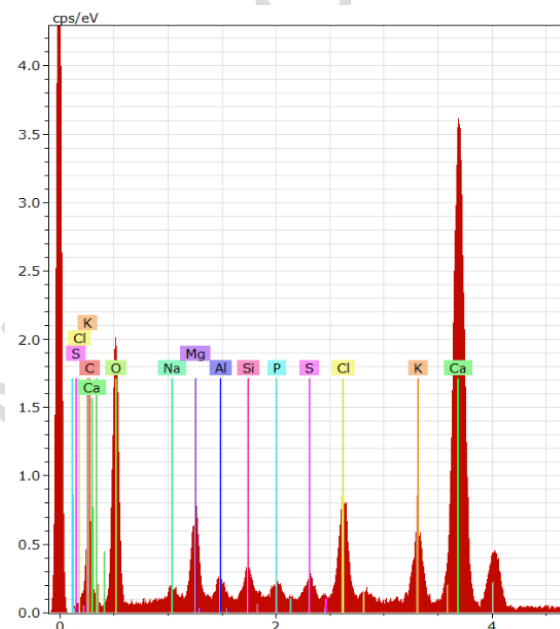227 Figure 1 b&c and Figure 1 d&f for FAD and FAC, respectively.
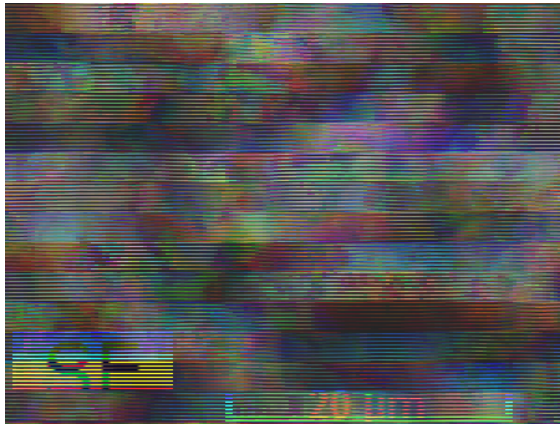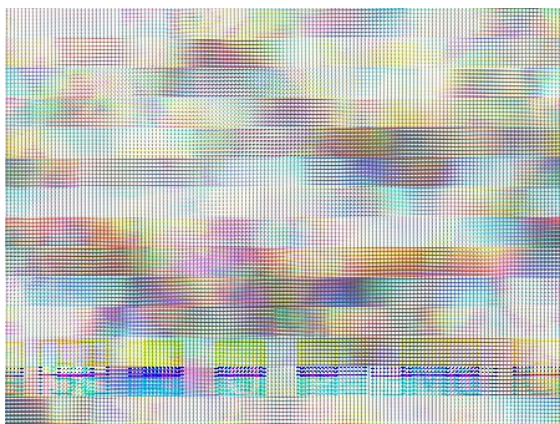
(a)

(b)
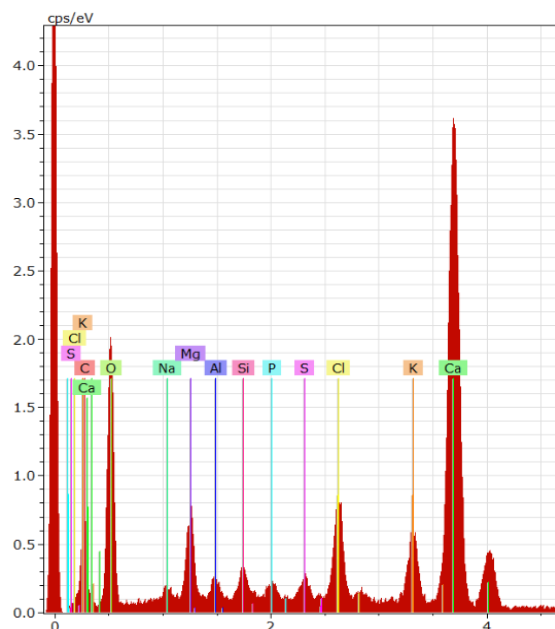
(c)

(d)

(e)   (f)

228   **Figure 1 -** FAD catalyst: SEM (a) and EDX (b and c); FAC catalyst: SEM (e) and EDX (d
229   and f).

230

231   Figure 2 displays the morphology of solid catalysts Dolomite C (Figure 2a) and Dolomite

232   CSC (Figure 2 b&c). The Dolomite C has a dense surface with heterogeneous distribution of

233   particle sizes (i.e., irregular size) and smooth appearance, which should be derived from

234   decarbonation process (calcination) of dolomite rock [27,34]. Sulfonation caused the

235   elongation of the crystalline structures as fibers due to sulfur compounds formation, as
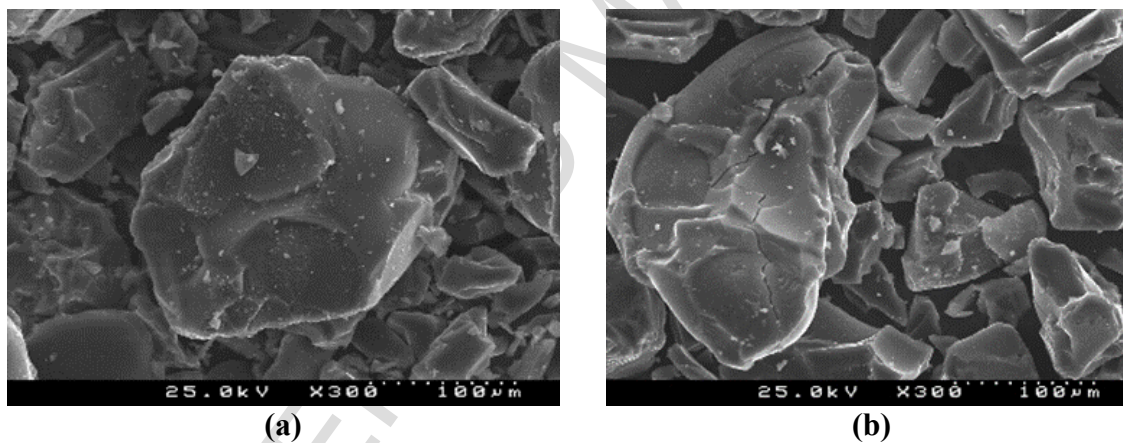
236   depicted in Figure 2 b&c.

| (a) | (b) | (c) |
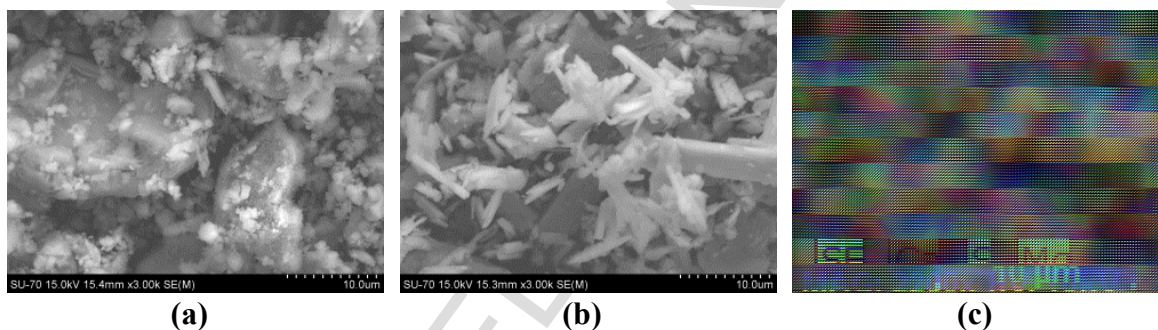
237   **Figure 2** - Dolomite C: SEM (a); Dolomite CSC: SEM (b) and EDX (c).

238   The catalyst prepared from eggshells CaO-SiO_2 exhibits large and regular blocks particles

239   (Figure 3a). The same was observed in the CaO-S-SiO_2 catalyst (image not shown) and one

240   infers that this morphology could be owed to the coverage of Si compounds on the CaO

241   surface (see Figure 3 b&c). More, the same effect was observed by Guanyi et al. (2015) [35].

242   As in the dolomitic catalysts, the sulfonation of CaO-SiO_2 solid also originated the formation

243   of crystalline structures as flat elongated fibers (Figure 3c) in this eggshells based material.

244   This phenomenon was also observed by Nurul et al. (2016) [36].

15

(a) **(b)** **(c)**
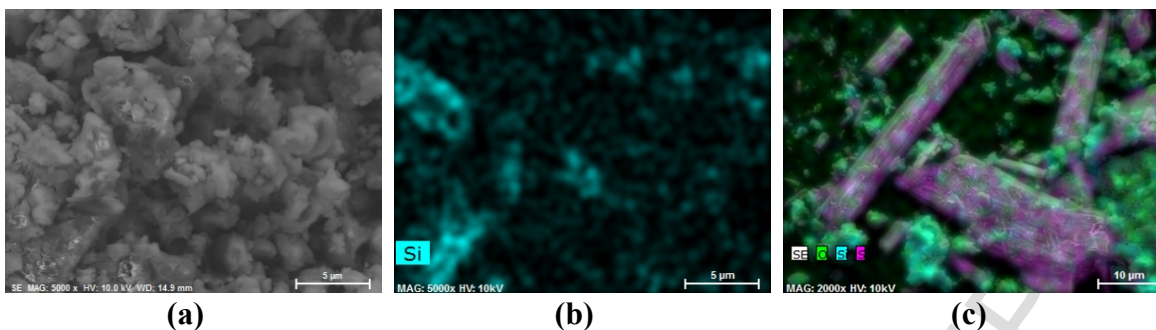
245 **Figure 3** - CaO-SiO$_2$: SEM (a); CaO-S-SiO$_2$: EDX (b) and (c).

246 The images taken for catalysts prepared from PET are shown in Figure 4, where it can be

247 seen irregular and flat surface with crevices. The sulfonation does not generate observable

248 significant differences in the morphology of this material, since particles have similar shapes

249 in both photos (a) and (b) of Figure 4. Similar behavior was observed in other studies

250 [29,37,38].

(a) **(b)**

251 **Figure 4** - SEM images of CA-PET (a) and CA-PET-S (b) catalysts.

252 **3.2.3 XRD analyses**

253 The XRD diffractograms of the fly ash catalysts are depicted in Figure 5a. The structure and

254 crystalline compounds of FAD and FAC are similar, being only their main differences the

16

255   area and the intensity of the peaks after calcination. The XRD pattern for FAD catalyst shows

256   clear diffraction peaks corresponding to calcium oxide (CaO) phase detected at $2\theta=32.2^{o}$,

257   37.4^{o}, 53.8^{o}, 65.2^{o}, and 67.5^{o}, calcium carbonate ($CaCO_3$-major component) phase detected

258   at $2\theta=23.3^{o}$, 29.6^{o}, 36.2^{o}, 39.7^{o}, 43.4^{o}, 47.8^{o}, 48.8^{o}, 56.9^{o}, 61.0^{o} and 65.0, potassium chloride

259   (KCl) phase detected at $2\theta=28.5^{o}$, 40.5^{o}, and silicon dioxide (SiO_2) phase detected at

260    $2\theta=20.9^{o}$, 26.7^{o}, 36.38^{o}, 39.46^{o}, 40.28^{o}, 50.2^{o}, 60.2^{o} and 68.5^{o}, among other components.

261   After the ash calcination, i.e. for FAC catalyst, $CaCO_3$ was transformed into CaO [17, 24,

262   28, 39, 40] and this is evident by the higher intensity of the corresponding peak. This latter

263   is the major component in FAC followed by the silicon dioxide (SiO_2).

(a)

(b)

(c)

(d)
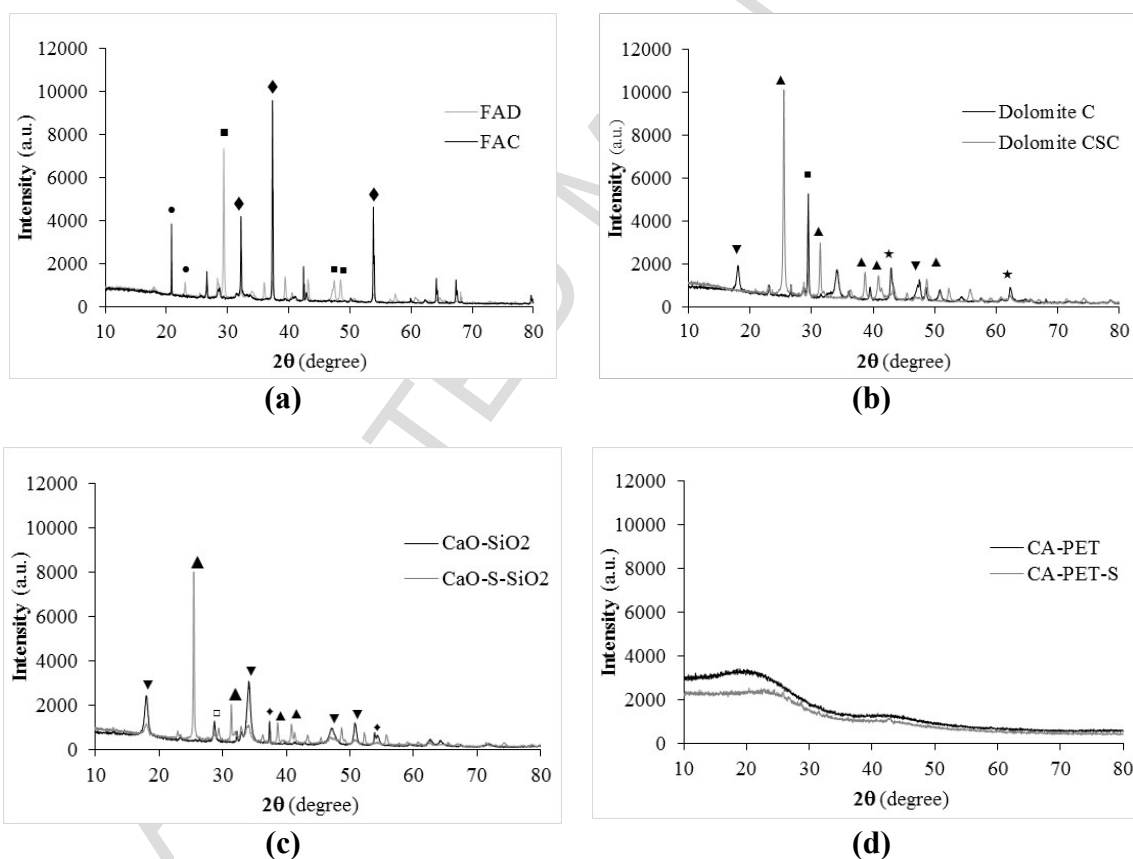
264 **Figure 5** - XRD patterns of catalysts: FAD and FAC (a), Dolomite C and Dolomite CSC
265 (b), CaO-SiO$_2$ and CaO-S-SiO$_2$ (c), and CA-PET and CA-PET-S (d). (• SiO$_2$, ■ CaCO$_3$, ♦
266 CaO, ▲ CaSO$_4$, ■ CaCO$_3$, ▼ Ca(OH)$_2$, ♦ CaO, □ Ca$_2$SiO$_4$ and ★ MgO).

267

268 Figure 5b shows the XRD of Dolomite C and Dolomite CSC catalysts. The presence of both

269 phases: CaO (2θ=32.2^o) and MgO (2θ=42.7^o) in the Dolomite C could promote the

270 transesterification reaction. Ca(OH)$_2$ (2θ=34.1^o) is part of the chemical composition of these

271 catalysts, its formation occurs readily upon an exposure of CaO to humidity of ambient,

272 resulting in a significant loss of the transesterification activity [34, 41]. It seems that

273 calcination time of dolomite rock was sufficient to decompose MgCO$_3$ in to MgO, but not

274 enough to convert completely the CaCO$_3$ in to CaO, since CaCO$_3$ is present (2θ=29.3^o) in

275 this catalyst after that thermal treatment; similar result was observed by Chawalit et al. (2010)

276 [42]. The sulfonation of Dolomite C originated new peaks in the diffractogram (of Dolomite

277 CSC), corresponding to calcium sulfate (CaSO$_4$-major component) at 2θ=25.6^o, 31.3^o, 38.6^o,

278 40.9^o, 48.6^o, 52.2^o, 55.8^o, and 65.0^o. As discussed previously, this treatment had also effects

279 on the basic and acid strengths of the solid catalyst due to the replacement of calcium

280 carbonate by calcium sulfate, which in turn could affect its catalytic activity.

281 The XRD patterns of the catalysts produced from eggshells are shown in Figure 5c. For CaO-

282 SiO$_2$ catalyst the peaks at 2θ =37.2^o, 64.2^o, 76.1^o and 2Θ=20.2^o, 33.4^o, 39.7^o, 55.3^o, 59.8^o

283 correspond to CaO and Ca(OH)$_2$, respectively. Besides, calcium silicate compounds

284 (Ca$_2$SiO$_4$) peaks appear at 2θ = 23.3^o, 26.2^o, 28.0^o 32.9^o, 35.1^o, 41.2^o due to the reaction of

285 Na$_2$SiO$_3$ with CaO and Ca(OH)$_2$ during the catalyst preparation process [28,43]. For the CaO-

286 S-SiO$_2$ catalyst new peaks have arose at 2θ =25.6^o, 31.3^o, 48.6^o and at 2θ =29.3^o,

18

287   corresponding to $CaSO_4$ and $CaCO_3$, respectively [44]. There are the three main compounds

288   that can be identified in the CaO-SiO_2 catalyst, namely: CaO, $Ca(OH)_2$ and Ca_2SiO_4. The

289   latter two are the most abundant, which means that part of the calcium existing in the

290   eggshells has reacted with Na_2SiO_3 to form calcium silicate [28, 43]. After CaO-SiO_2

291   sulfonation, the hydroxides and silicates of calcium were mainly converted into $CaSO_4$, the

292   predominant compound in this catalyst.

293   Finally, the XRD diffractograms of catalysts prepared from PET are depicted in Figure 5d.

294   Both diffractograms exhibit a broad diffraction peaks indicating an amorphous carbons,

295   C(002) and C(101), which is composed of the oriented random fashion of carbon sheets.

296   Thus, a high content of non-graphitic carbon structure is comprised of both samples. Fadhil

297   et al. (2016) [29] and Chang et al. (2015) [45] observed that these kind of carbons have

298   oriented random fashion sheets. In short, both catalysts prepared from PET have high content

299   of non-graphitic carbon.

300   **3.2.4   FTIR analyses**

301   The FTIR spectra of all catalysts prepared in this work are shown in Figure 6. The FTIR

302   spectrum of FAD (Figure 6 a) shows the major absorption broad band at 1408.1 cm^{-1} and

303   minor absorption bands at 875.5 and 711.2 cm^{-1}, which correspond to the asymmetric

304   stretching and to out-of-plane band and in-plane band vibration modes of carbonate (CO_3^{-2})

305   group, respectively. This result confirms the presence of $CaCO_3$ in FAD, detected by XRD.

306   PO_4^{-3} and Si-O components (silica phosphates) show broad bands in the region between

307   1100.5 and 911.6 cm^{-1}; the same was observed by Maneerung et al. (2015) and Sharma et al.

308   (2012) but using bottom ash waste arising from woody biomass gasification and wood ash

309   from the *Acacia nilotica* (babul), respectively. Moreover, the absorption sharp band at 3643

310   cm^{-1}, which is attributed to -OH band, was observed for both catalysts (calcined and

311   uncalcined). This band is an evidence of water absorption on the CaO surface producing

312   $Ca(OH)_2$ [46].

(a)   **(b)**

(c)   **(d)**
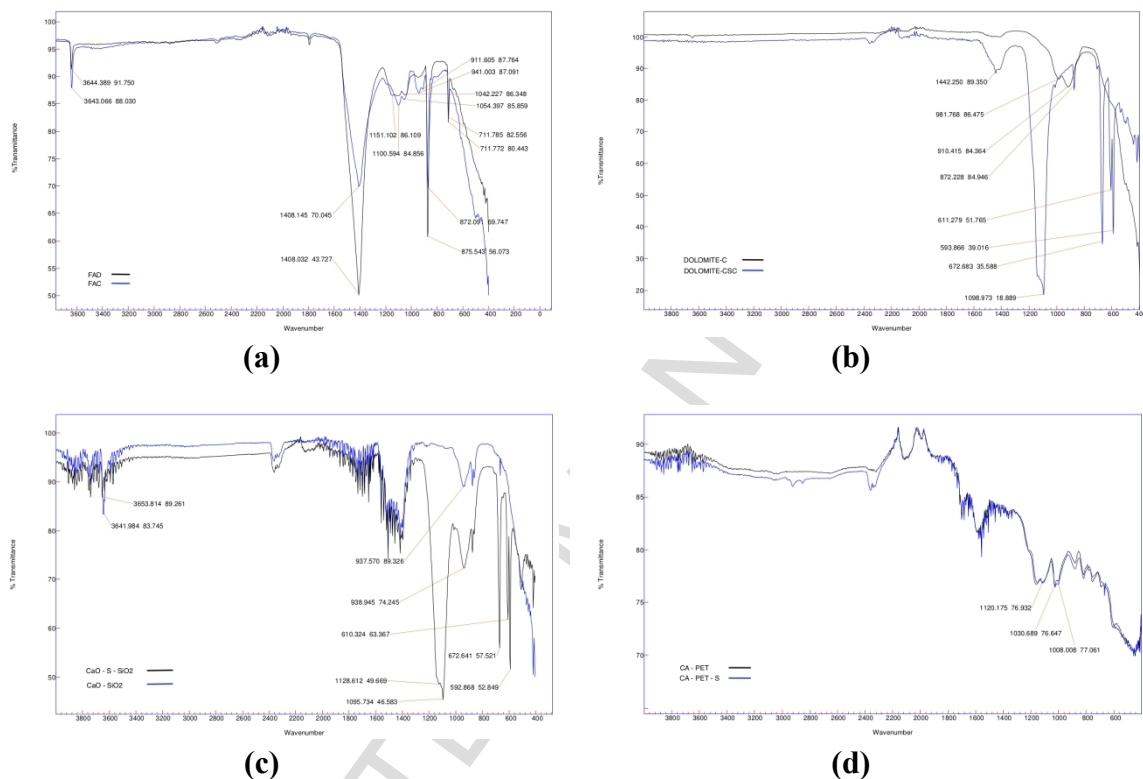
313   **Figure 6 -**   FTIR spectra of catalysts: FAD and FAC (a), Dolomite C and Dolomite CSC
314   (b), $CaO-SiO_2$ and $CaO-S-SiO_2$ (c), and CA-PET and CA-PET-S (d).

315

316   The typical transmittance FTIR spectra of the Dolomite C and Dolomite CSC are shown in

317   Figure 6b. The bands at 1442.2 and 1438 cm^{-1} can be assigned to the symmetric and

318   asymmetric stretching vibrations of O–C–O bonds of unidentate carbonate at the surface of

319   the calcium–magnesium oxide in both dolomitic catalysts [34, 47]. The band 872.2 cm^{-1}

20

320 arises also from these carbonates groups. For the Dolomite CSC, the peaks at 1098.9, 672.6,

321 611.2 and 593.8 cm^{-1} are attributed to the functional group SO_4^{-2} of calcium sulfate (major

322 component) [48, 49].

323 Regarding the FTIR spectra of CaO-SiO_2 and CaO-S-SiO_2 catalysts (Figure 6c), one

324 observes nearby absorption bands, such as at 3641.9 and 3653.8 cm^{-1} that correspond to the

325 stretching O-H due to physisorption of water on the solid surface. The spectra show

326 matching bands namely at 937.5 and 938.9 cm^{-1}, which belong to Si-O symmetric elongation

327 vibrations and Si–O–Ca [50, 51]. The absorption band at 1128.6 cm^{-1} could be attributed to

328 O–Si–O bond of silicate compounds [52]. For CaO-S-SiO_2 catalyst, the bands at 1095.7,

329 672.6, 610.3 and 592.8 cm^{-1} are attributed to the stretching vibrations of S=O on the group

330 SO_4^{-2} of calcium sulfate [48, 49].

331 Concerning the FTIR spectra of CA-PET and CA-PET-S catalysts (Figure 6 d), both are

332 similar in respect to the position of their bands. The absorption bands observed at 1008, 1030

333 and 1120 cm^{-1} are assigned to the symmetric stretching vibrations of S=O as result of

334 inducing the SO_3H group [45, 53]. These evidences indicate a successful incorporation of

335 SO_3H functional groups in the carbon framework.

3.3 Catalysts performance

337 The performance of the catalysts prepared from waste materials was assessed through the

338 esterification and transesterification reaction yields, in the conversion of RPO and WCO

339 mixtures to FAME. The results are plotted in Figure 7 for FAME yield (Eq.4) and FFA

340 conversion (Eq.5). As the WCO percentage in the reaction mixture increases two main

341 conclusions are withdrawn by an overview of Figure 7, namely:

342 ▪ A decrease of FAME yield for catalysts with moderate or high basic strength. This
343 can be due to the neutralization of their basic catalyst sites, as stated by Kaur M. et
344 al. (2011) [54] and Kouzu M. et al. (2008) [55];
345 ▪ An increase (or maintenance, for FAD) of FFA conversion.

346 Thus, the presence of FFA in the reaction mixture favours their conversion to FAME but has

347 a negative effect on transesterification reaction yield.

348 A more detailed analysis of each catalyst group shows that the fly ash catalysts (Figure 7

349 a&b) have the highest FAME yield for all oil blends tested. One of the best performances (of

350 all catalysts) in FFA conversion is also related to one of these catalysts, the FAD, achieving

351 values above 96% for all mixtures. However, rising the WCO in the reaction mixture

352 decreases the FAME yield in ca. 30 to 35%, being the FAC performance the most affected.

353 Among the two ash based catalysts, the FAC is the one that has a worse performance in both

354 FAME yield and FFA conversion. This evidence may be due to changes in surface

355 morphology (sintering processes) and decrease of both crystalline phases and active

356 functional groups on the surface for the calcined catalyst, as observed by XRD and FTIR.

357 Additionally, the most abundant compound in FAD is $CaCO_3$ and in FAC is CaO, which may

358 be another reason for the observed differences in performance. However, as the amount of

359 WCO in the blend increases these differences in performance of the catalyst decrease

360 significantly.

361   Despite of the low acid strength of both catalysts (6.8≤ pKa <7.2), the FAD roughly converts

362   all FFA present in the initial reaction mixture and the FAC increases its performance as the

363   WCO percentage rises, achieving ca. 86% of conversion for 100%wt. of WCO (M5).

364   Summing up, it is reasonable to conclude that these catalysts have a bifunctional character,

365   especially the FAD which enables attaining FAME yield and FFA conversions around 95%

366   for WCO blends of 25%wt. (M2).

367

(a)   (b)

(c)   (d)

(e) **(f)**

(g) **(h)**
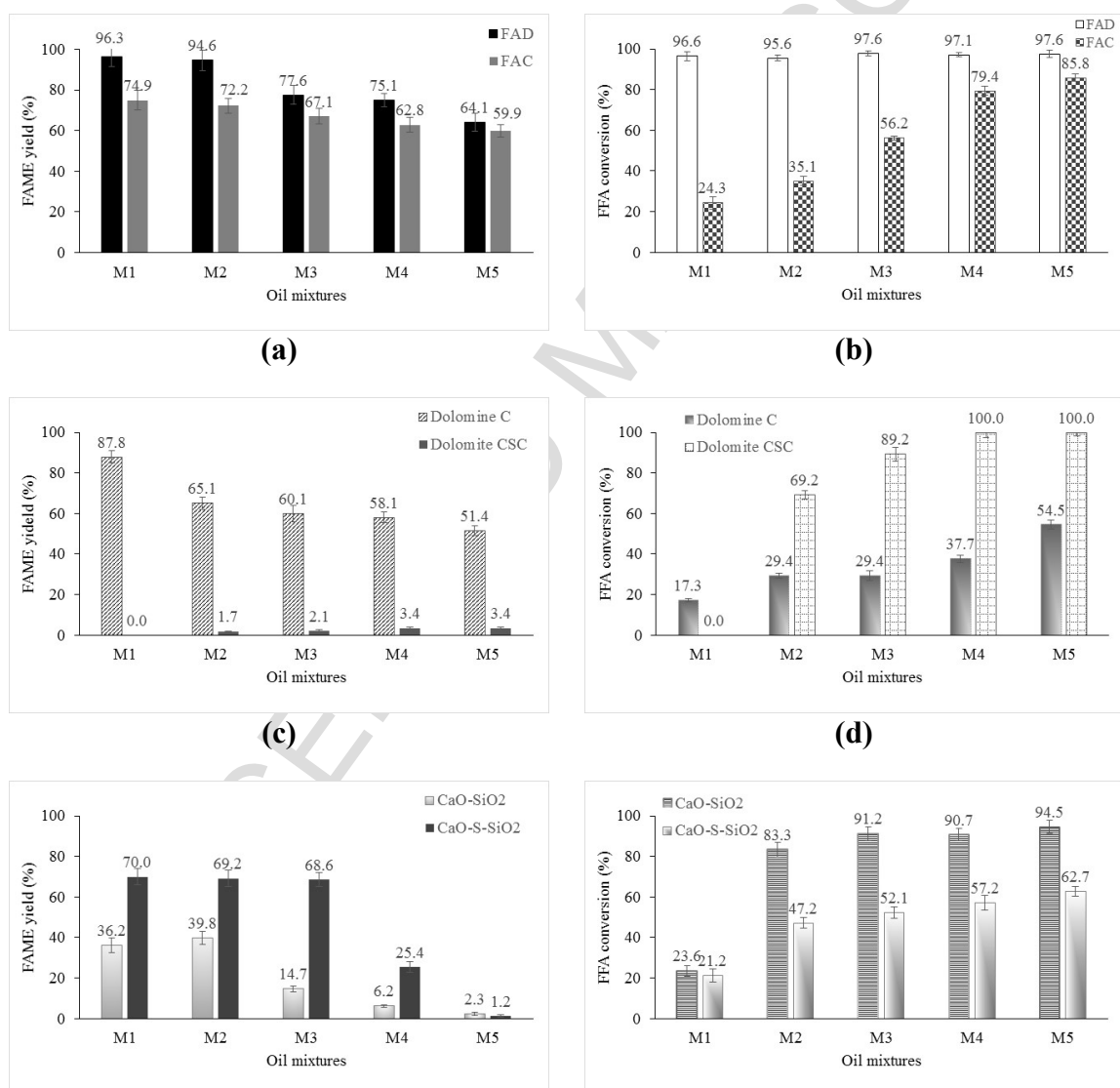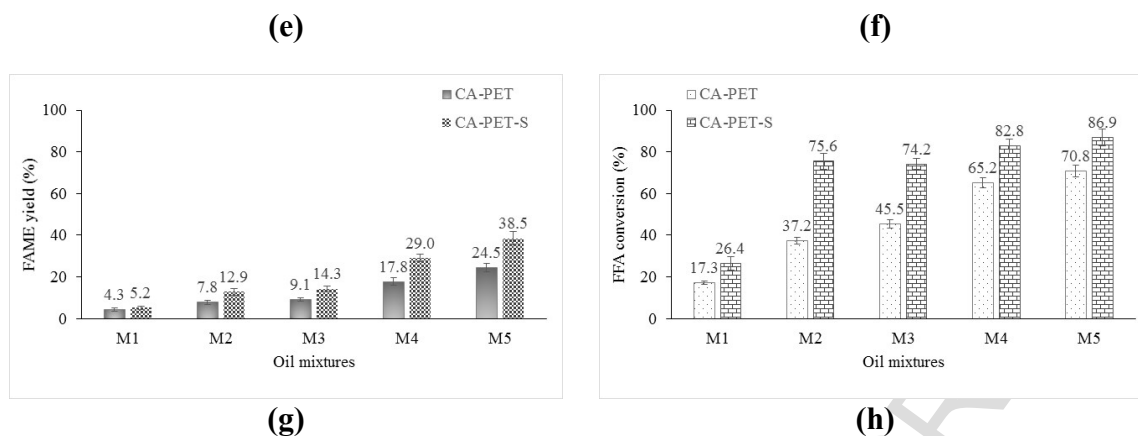
368 **Figure 7 -** Performance in terms of FAME yield and FFA conversion of catalysts: FAD and
369 FAC (a) and (b), Dolomite C and Dolomite CSC (c) and (d), CaO-SiO$_2$ and CaO-S-SiO$_2$ (e)
370 and (f), and CA-PET and CA-PET-S(g) and (h), for several RPO:WCO mixtures.

371

372 The FAME yields and FFA conversions attained using Dolomite catalysts are summarized

373 in the Figure 7c and Figure 7d, respectively. Dolomite C has the highest basic strength (12.2≤

374 pKa <15), but this is not reflected in higher FAME yields. Furthermore, in comparison to ash

375 catalysts, Dolomite C has higher surface area, pore volume and pore diameter, and all these

376 features do not seem to be sufficient to give a better performance to this catalyst. Thus,

377 chemical composition of the catalyst could have a stronger influence than those physical

378 characteristics. The highest FAME yield achieved by this catalyst is ca. 88% for M1, and

379 decreases 37% for the mixture with higher acid value (M5). With regard to FFA conversion,

380 the values attained are consistent with the low acid strength exhibited by this catalyst, i.e.,

381 Dolomite C has a low acid strength and consequently is a weak catalyst of esterification

382 reaction, so the FFA conversion values reached are one of the lowest registered (for each oil

383 mixture).

24

384 The sulfonation and subsequent calcination of Dolomite C, giving rise to Dolomite CSC, has

385 strongly affected its ability to catalyze the transesterification reaction, nearly annulling it.

386 This could be due to the decrease of basic strength (by neutralization) and/or to the decrease

387 of pore diameter, which in turn increases the diffusion limitations for long alkyl chain

388 molecules (e.g., triglycerides). However, this treatment has improved the performance of this

389 material for catalyzing the esterification reaction, reaching conversions of 100% for oil

390 mixtures with the highest acid values (M4 and M5) tested in this work. The moderate acid

391 character of this catalyst ($6.1 \leq pKa < 6.8$) and the functional groups on its surface (group SO_4^{-2}

392) could be the driving force of its performance in converting FFA to FAME.

393 The data concerning the performance eggshell catalysts ($CaO-SiO_2$ and $CaO-S-SiO_2$) are

394 plotted in the Figure 7 (e and f). The FAME yield are negatively affected by the initial acid

395 value of the oil mixtures, achieving the lowest values (of all catalysts) for M5. The highest

396 yield levels reached was 70% for M1 in $CaO-SiO_2$ catalyst and 40% for M2 in $CaO-S-SiO_2$;

397 similar results were obtained by Guanyi C. et al. (2015) [28]. The sulfonation and calcination

398 of $Ca-SiO_2$ material increases the FAME yield, possibly due to the formation of new active

399 phases such as calcium sulfate ($CaSO_4$) and calcium carbonate formed from calcium

400 hydroxide ($Ca(OH)_2$) and calcium silicate (Ca_2SiO_4), as shown in the Figure 5c, which have

401 low activity towards the transesterification reaction. Relating to the performance of eggshells

402 based catalysts to converting the FFA to FAME, one can say that as WCO percentage in the

403 oil mixture increases the higher is the conversion, being the $Ca-SiO_2$ catalyst the best one.

404 This finding is in agreement with the acid strength of that catalyst ($Ca-SiO_2$), which is one of

405 the highest ($3.8 \leq pKa < 4.7$) observed in this work.

25

406   Compared to the several catalysts discussed above, those produced from PET exhibit an

407   inverse trend over the FAME yield (Figure 7 g). It was registered an increase of yield as the

408   amount of FFA in the oil mixtures rises, but the higher values attained were low, i.e., ca. 25%

409   and 39% for M5 in CA-PET and CA-PET-S, respectively. This result can be explained

410   considering the lack of basic strength in these catalysts (see Table 3). In fact, PET catalysts

411   only have an acid character, being CA-PET-S the catalyst with the most acidic character

412   produced in this work (3.8 ≤pKa <4.7). Though, they do not have the best performance in the

413   esterification reaction catalysis. In Figure 7 h one observes that the FFA conversions

414   increases as the acid value of oil mixture rises, achieving the maximum values of ca.71% and

415   87% for M5 in CA-PET and CA-PET-S, respectively. Thus, although these catalysts have

416   the largest specific surface area, the largest pore volume and one of the highest acidic

417   strenghts, this does not seem to be enough to make them the best catalysts for the

418   esterification reaction. A plausible reason for this may lie in the fact that they have the

419   smallest pore size observed among the catalyst developed in this work. In addition, among

420   the two PET catalysts, CA-PET-S is the one that has a better performance in the catalysis of

421   both esterification and transesterification reactions.

422   **4   Conclusions**

423   In the present study, efficient heterogeneous catalysts were successfully prepared from solid

424   waste materials for biodiesel production by transesterification and esterification, using

425   mixtures of refined palm oil and waste cooking oil in different ratios and methanol. The

426   results demonstrate that all the catalysts evaluated have different catalytic performances. The

427 better catalyst for catalyzing simultaneous both transesterification and esterification

428 reactions, i.e., having a bifunctional character, was biomass fly ash dried (FAD), achieving

429 yields and conversions above 95% for a blend of up to 25%wt. of WCO.

430 The catalyst produced from dolomite rock did not have a strong bifunctional character. They

431 showed good performances in catalyzing the transesterification and esterification reactions,

432 but not simultaneously. Indeed, the sulfonation of Dolomite C was aimed at increasing its

433 acidic strength so as to give it the potential to catalyze the esterification reaction. However,

434 that treatment strongly affected that ability, practically canceling it. In further procedures,

435 the sulfonation stage should be more lenient.

436 The sulfonation of material prepared from eggshells improved its ability for catalyzing the

437 transesterification reaction, however the maximum values attained do not exceed 70% of

438 yields. On the other hand, this treatment worsened the performance of this catalyst in FFA

439 conversion.

440 Regarding the catalysts produced from PET, the results showed that they are good candidates

441 for catalyzing the esterification reaction of high acid value feedstocks.

442 In short, none of the catalysts produced in this work has both high basic and acidic strengths

443 and the only one that has these two strengths balanced (on a moderate level) is the Dolomite

444 CSC. However, the catalyst that exhibited a bifunctional character was undoubtedly FAD,

445 which means this material can be directly and immediately used from the electrostatic

446 precipitator equipment located at the biomass thermal power-plant, as its moisture content is

447 very low, with subsequent economic benefits.

448 By the exploitation of residual feedstocks (e.g., WCO) and the use of waste based catalysts,

449 this work gives a contribution to make the biodiesel production a low cost, affordable and

450 sustainable process, and simultaneously minimizing the environmental burdens traditionally

451 inherent to the management of those wastes. Therefore, an awareness should be created so

452 that any material that is deemed to be waste could be exploited for usage in this or other

453 applications, thereby implementing the principles of circular economy.

Acknowledgments

References

461 [1] Information from http://www.eia. gov/forecasts/ieo/ (accessed on [accessed 06.12.16].

462 [2] Leung DYC, Wu X, Leung MKH. A review on biodiesel production using catalyzed

463 transesterification, Applied Energy 87 (2010) 1083–1095.

464 [3] Peng-Lim Boey, Gaanty Pragas Maniam, Shafida Abd Hamid. Biodiesel production via

465 transesterification of palm olein using waste mud crab (Scylla serrata) shell as a

466 heterogeneous catalyst. Bioresource Technology 100 (2009) 6362–6368.

467　[4] Muhammad F, Anita R, Abdul N. Biodiesel production from low FFA waste cooking oil

468　using heterogeneous catalyst derived from chicken bones. Renewable Energy 76 (2015) 362–

469　368.

470　[5] Nasar Mansira, Siow Hwa Teo, Umer Rashidc, Mohd Izham Saimana, Yen Ping Tan, G.

471　Abdulkareem Alsultana, Yun Hin Taufiq-Yap. Modified waste egg shell derived bifunctional

472　catalyst for biodiesel production from high FFA waste cooking oil. A review. Renewable and

473　Sustainable Energy Reviews 82 (2018) 3645–3655.

474　[6] Irma N, Gaanty M, Noor H, Mashitah Y, Shangeetha G. Potential of feedstock and

475　catalysts from waste in biodiesel preparation: A review. Energy Conversion and Management

476　74 (2013) 395–402.

477　[7] Demirbas A. Biodiesel from waste cooking oil via base-catalytic and supercritical

478　methanol transesterification. Energy Conversion and Management. 50 (2009) 923–927.

479　[8] Jein-Wen Chen, Shu-Li Wang, Dannis Paul Hsientang Hsieh, Hsi-Hsien Yang, Hui-Ling.

480　Carcinogenic potencies of polycyclic aromatic hydrocarbons for back-door neighbors of

481　restaurants with cooking emissions. Science of the Total Environment 417–418 (2012) 68–

482　75.

483　[9] Farooq M, Ramli A, Subbarao D. Biodiesel production from waste cooking oil using

484　bifunctional heterogeneous solid catalysts. J Clean Prod 59 (2013) 131–140.

485　[10] ICONTEC, Norma Técnica Colombiana NTC.218. Grasas y aceites vegetales y

486　animales. Determinación del índice de acidez y de la acidez., Instituto Colombiano de

487　Normas Técnicas y Certificación, Bogotá, D.C., 2011.

488 [11] ICONTEC, Norma Técnica Colombiana NTC.336. Grasas y aceites animales y

489 vegetales. Método de determinación de la densidad-Masa por volumen convencional.

490 Instituto Colombiano de Normas Técnicas y Certificaciones, Bogotá, D.C., 2002.

491 [12] ICONTEC, Norma Técnica Colombiana NTC 335. Grasas y aceites animales y

492 vegetales. Determinación del índice de saponificación, Instituto Colombiano de Normas

493 Técnicas y Certificación, Bogotá, D.C., 1998.

494 [13] ASTM International, especificaciones estándar e instrucciones de funcionamiento para

495 viscosímetros cinemáticos capilares de vidrio., Annu. B. Stand de ASTM. (2009) 1–24.

496 [14] ASTM International, Método de prueba estándar para la viscosidad cinemática de

497 líquidos transparentes y opacos (y cálculo de la viscosidad dinámica), 2010.

498 [15] UNE-EN 14103, Norma Española. Determinación de los contenidos de éster y éster

499 metílico de ácido linoleico, 2003.

500 [16] Wan Nor Nadyaini Wan Omar, Nor Aishah Saidina Amin. Biodiesel production from

501 waste cooking oil over alkaline modified zirconia catalyst. Fuel Processing Technology 92

502 (2011) 2397–2405.

503 [17] Bijaya K. Uprety, Wittavat Chaiwong, Chinomnso Ewelike, Sudip K. Rakshit. Biodiesel

504 production using heterogeneous catalysts including wood ash and the importance of

505 enhancing byproduct glycerol purity. Energy Conversion and Management 115 (2016) 191–

506 199.

507 [18] Jibrail Kansedo, Keat Teong Lee, Subhash Bhatia. Cerbera odollam (sea mango) oil as

508 a promising non-edible feedstock for biodiesel production. Fuel 88 (2009) 1148–1150.

509   [19] S.P. Singh, Dipti Singh. Biodiesel production through the use of different sources and

510   characterization of oils and their esters as the substitute of diesel: A review. Renewable and

511   Sustainable Energy Reviews 14 (2010) 200–216.

512   [20] Wan Nor Nadyaini Wan Omar, Nor Aishah Saidina Amin. Optimization of

513   heterogeneous biodiesel production from waste cooking palm oil via response surface

514   methodology. Biomass and bioenergy 35 (2011) 1329–1338.

515   [21] Man Kee Lam, Keat Teong Lee. Accelerating transesterification reaction with

516   biodiesel as co-solvent: A case study for solid acid sulfated tin oxide catalyst. Fuel 89

517   (2010) 3866–3870.

518   [22] M.R. Avhad, J.M. Marchetti. A review on recent advancement in catalytic materials

519   for biodiesel production. Renewable and Sustainable Energy Reviews 50 (2015) 696–718.

520   [23] Li Y, Zhang X, Sun L, Zhang J, Xu H. Fatty acid methyl ester synthesis catalyzed by

521   solid superacid catalyst. Appl Energy 87 (2010) 156–159.

522   [24] Thawatchai Maneerung, Sibudjing Kawi, Chi-Hwa Wang. Biomass gasification bottom

523   ash as a source of CaO catalyst for biodiesel production via transesterification of palm oil.

524   Energy Conversion and Management 92 (2015) 234–243.

525   [25] Man Kee Lam, Keat Teong Lee, Abdul Rahman Mohamed. Sulfated tin oxide as solid

526   superacid catalyst for transesterification of waste cooking oil: An optimization study.

527   Applied Catalysis B: Environmental 93 (2009) 134–139.

528   [26] K. Jacobson, R. Gopinath, L.C. Meher, A.K. Dalai. Solid acid catalyzed biodiesel

529   production from waste cooking oil, Applied Catalysis B: Environmental 85 (2008) 86–91.

31

530   [27] Boonyawan Yoosuk, Parncheewa Udomsap, Buppa Puttasawat. Hydration –dehydration

531   technique for property and activity improvement of calcined natural dolomite in

532   heterogeneous biodiesel production: Structural transformation aspect. Applied Catalysis A:

533   General 395 (2011) 87–94.

534   [28] Guanyi Chen, Rui Shan, Shangyao Li, Jiafu Shi. A biomimetic silicification approach

535   to synthesize CaO–SiO$_2$ catalyst for the transesterification of palm oil into biodiesel. Fuel

536   153 (2015) 48–55.

537   [29] Abdelrahman B. , Akram M. Aziz, Marwa H. Al-Tamer. Biodiesel production from

538   Silybum marianum L. seed oil with high FFA content using sulfonated carbon catalyst for

539   esterification and base catalyst for transesterification. Energy Conversion and Management

540   108 (2016) 255–265.

541   [30] M.E. Borges, L. Díaz. Recent developments on heterogeneous catalysts for biodiesel

542   production by oil esterification and transesterification reactions: A review. Renewable and

543   Sustainable Energy Reviews 16 (2012) 2839– 2849.

544   [31] Avelino Corma. From microporous to mesoporous molecular sieve materials and their

545   use in catalysis. Chemical Reviews 97 (1997) 2373−2419.

546   [32] Wilson Wei Sheng Ho, Hoon Kiat Ng, Suyin Gan, Sang Huey Tan. Evaluation of palm

547   oil mill fly ash supported calcium oxide as a heterogeneous base catalyst in biodiesel

548   synthesis from crude palm oil. Energy Conversion and Management 88 (2014) 1167–1178.

549   [33] N. Muthukumaran, C.G. Saravanan, S. Prasanna Raj Yadav, R. Vallinayagam, S.

550   Vedharaj, W.L. Roberts. Synthesis of cracked Calophyllum inophyllum oil using fly ash

551   catalyst for diesel engine application. Fuel 155 (2015) 68–76.

552   [34] Leandro Marques Correia, Natália de Sousa Campelo, Denise Sousa Novaes,

553   Célio Loureiro Cavalcante Jr., Juan Antonio Cecilia, Enrique Rodríguez-Castellón,

554   Rodrigo Silveira Vieira. Characterization and application of dolomite as catalytic precursor

555   for canola and sunflower oils for biodiesel production. Chemical Engineering Journal 269

556   (2015) 35–43.

557   [35] Guanyi Chen, Rui Shan, Shangyao Li, Jiafu Shi. A biomimetic silicification approach

558   to synthesize CaO–SiO$_2$ catalyst for the transesterification of palm oil into biodiesel. Fuel

559   153 (2015) 48–55.

560   [36] Nurul Hajar Embong, Gaanty Pragas Maniam, Mohd Hasbi Ab. Rahim, Keat Teong Lee

561   c, Donald Huisingh. Utilization of palm fatty acid distillate in methyl esters preparation using

562   SO$_4^{2-}$/TiO$_2$-SiO$_2$ as a solid acid catalyst. Journal of Cleaner Production 116 (2016) 244–248.

563   [37] Zahra Hajamini, Mohammad Amin Sobati, Shahrokh Shahhosseini,Barat Ghobadian.

564   Waste fish oil (WFO) esterification catalyzed by sulfonated activated carbon under

565   ultrasound irradiation. Applied Thermal Engineering 94 (2016) 141–150.

566   [38] F.A. Dawodu, O. Ayodele, J. Xin, S. Zhang, D. Yan. Effective conversion of non-edible

567   oil with high free fatty acid into biodiesel by sulphonated carbón catalyst. Appl. Energy 114

568   (2014) 819–826.

569 [39] Wilson Wei Sheng Ho, Hoon Kiat Ng, Suyin Gan. Development and characterisation of

570 novel heterogeneous palm oil mill boiler ash-based catalysts for biodiesel production.

571 Bioresource Technology 125 (2012) 158–164.

572 [40] Meeta Sharma, Arif Ali Khan, S.K. Puri, D.K. Tuli. Wood ash as a potential

573 heterogeneous catalyst for biodiesel synthesis. biomass and bioenergy 41 (2012) 94–106.

574 [41] Siyada Jaiyen, Thikumporn Naree , Chawalit Ngamcharussrivichai. Comparative study

575 of natural dolomitic rock and waste mixed seashells as heterogeneous catalysts for the

576 methanolysis of palm oil to biodiesel. Renewable Energy 74 (2015) 433–440.

577 [42] Chawalit Ngamcharussrivichai, Pramwit Nunthasanti, Sithikorn Tanachai, Kunchana

578 Bunyakiat. Biodiesel production through transesterification over natural calciums. Fuel

579 Processing Technology 91 (2010) 1409–1415.

580 [43] F.H.G. Leite, T.F. Almeida, R.T. Faria Jr, J.N.F. Holanda. Synthesis and

581 characterization of calcium silicate insulating material using avian eggshell waste. Ceramics

582 International 43 (2017) 4674–4679.

583 [44] O. Nur Syazwani, M. Lokman Ibrahim, Wahyudiono, Hideki Kanda, Motonobu Goto,

584 Y.H. Taufiq-Yap. Esterification of high free fatty acids in supercritical methanol using

585 sulfated angel wing shells as catalyst. J. of Supercritical Fluids 124 (2017) 1–9.

586 [45] Binbin Chang, Yanzhen Guo, Hang Yin, Shouren Zhang, Baocheng Yang. Synthesis of

587 sulfonated porous carbon nanospheres solid acid by a facile chemical activation route.

588 Journal of Solid State Chemistry 221 (2015) 384–390.

589   [46] Peng-Lim Boey, Shangeetha Ganesan, Sze-Xooi Lim, Sau-Lai Lim, Gaanty Pragas

590   Maniam, Melati Khairuddean. Utilization of boiler ashes catalyst for transesterification of

591   palm olein. Energy 36 (2011) 5791–5796.

592   [47] Y.T. Algoufi, G. Kabir, B.H. Hameed. Synthesis of glycerol carbonate from biodiesel

593   by-product glycerol over calcined dolomite. Journal of the Taiwan Institute of Chemical

594   Engineers 70 (2017) 179–187.

595   [48] Bao Konga, Jie Yu, Keith Savino, Yigang Zhu, Baohong Guan. Synthesis of alpha-

596   calcium   sulfate   hemihydrate   submicron-rods   in   water/n-hexanol/CTAB   reverse

597   microemulsion. Colloids and Surfaces A: Physicochem. Eng. Aspects 409 (2012) 88–93.

598   [49] Yuzeng Zhao, Lingling Jia, Kuaiying Liu, Pan Gao, Honghua Ge, Lijun Fu. Inhibition

599   of calcium sulfate scale by poly (citric acid). Desalination 392 (2016) 1–7.

600   [50] Guan-Yi Chen, Rui Shan, Jia-Fu Shi, Bei-Bei Yan. Transesterification of palm oil to

601   biodiesel using rice husk ash-based catalysts. Fuel Processing Technology 133 (2015) 8–13.

602   [51] Jutika Boro, Ashim J. Thakur, Dhanapati Deka. Solid oxide derived from waste shells

603   of Turbonilla striatula as a renewable catalyst for biodiesel production. Fuel Processing

604   Technology 92 (2011) 2061–2067.

605   [52] H. Amani, M. Asif, B.H. Hameed. Transesterification of waste cooking palm oil and

606   palm oil to fatty acid methyl ester using cesium-modified silica catalyst. Journal of the

607   Taiwan Institute of Chemical Engineers 58 (2016) 226–234.

608   [53] Rong Xing, Yueming Liu, Yong Wang, Li Chen, Haihong Wu, Yongwen Jiang,

609   Mingyuan He, Peng Wu. Active solid acid catalysts prepared by sulfonation of carbonization-

35

610   controlled mesoporous carbon materials. Microporous and Mesoporous Materials 105 (2007)

611   41–48.

612   [54] Kaur M, Ali A. Lithium ion impregnated calcium oxide as nano catalyst for the biodiesel

613   production from karanja and Jatropha oils. Renewable Energy 36 (2011) 2866–2871.

614   [55] Kouzu M, Kasuno T, Tajika M, Sugimoto Y, Yamanaka S, Hidaka J. Calcium oxide as

615   a solid base catalyst for transesterification of soybean oil and its application to biodiesel

616   production. Fuel 87 (2008) 2798–2806.

617

- Dried biomass fly ash is a bifunctional character catalyst in the FAME production
- Dolomite based catalysts are good in trans/esterification reactions (separately)
- Sulfonation of eggshells improves its performance in transesterification catalysis
- Activated carbon produced from PET are able to catalyze esterification reaction